

4. Rue, E. L. & Bruland, K. W. Complexation of iron(III) by natural organic ligands in the Central North Pacific as determined by a new competitive ligand equilibration/adsorptive cathodic stripping voltammetric method. *Mar. Chem.* **50**, 117–138 (1995).
5. Witter, A. E. & Luther, G. W. Variation in Fe-organic complexation with depth in the Northwestern Atlantic Ocean as determined using a kinetic approach. *Mar. Chem.* **62**, 241–258 (1998).
6. Hutchins, D. A. in *Progress in Physiological Research* Vol. 11 (eds Chapman, D. & Round, F.) 1–49 (Biopress, Bristol, 1995).
7. Wilhelm, S. W. Ecology of iron-limited cyanobacteria: a review of physiological responses and implications for aquatic systems. *Aquat. Microbial Ecol.* **9**, 295–303 (1995).
8. Butler, A. Acquisition and utilization of transition metal ions by marine organisms. *Science* **281**, 207–210 (1998).
9. Granger, J. & Price, N. M. The importance of siderophores in iron nutrition of heterotrophic marine bacteria. *Limnol. Oceanogr.* **44**, 541–555 (1999).
10. Jones, G. J., Palenik, B. P. & Morel, F. M. M. Trace metal reduction by phytoplankton: the role of plasmalemma redox enzymes. *J. Phycol.* **23**, 237–244 (1987).
11. Weger, H. G. Ferric and cupric reductase activities in the green alga *Chlamydomonas reinhardtii*: experiments using iron-limited chemostats. *Planta* **207**, 377–384 (1999).
12. Reid, R. T., Live, D. H., Faulkner, D. J. & Butler, A. A siderophore from a marine bacterium with an exceptional ferric iron affinity constant. *Nature* **366**, 455–458 (1993).
13. Hutchins, D. A. & Bruland, K. W. Grazer-mediated regeneration and assimilation of Fe, Zn and Mn from planktonic prey. *Mar. Ecol. Prog. Ser.* **110**, 259–269 (1994).
14. Gobler, C. J. *et al.* Elemental release and bioavailability following viral lysis of a marine chrysophyte. *Limnol. Oceanogr.* **42**, 1492–1504 (1997).
15. Strom, S. L. Production of phaeopigments by marine protozoa: results of laboratory experiments analyzed by HPLC. *Deep Sea Res.* **1** **40**, 57–80 (1993).
16. Head, E. J. H. & Harris, L. R. Feeding selectivity by copepods grazing on natural mixtures of phytoplankton determined by HPLC analysis of pigments. *Mar. Ecol. Prog. Ser.* **110**, 75–83 (1994).
17. McCarthy, M., Pratum, T., Hedges, J. & Benner, R. Chemical composition of dissolved organic nitrogen in the sea. *Nature* **390**, 150–154 (1997).
18. Hudson, R. J. M. & Morel, F. M. M. Iron transport in marine phytoplankton: Kinetics of cellular and medium coordination reactions. *Limnol. Oceanogr.* **35**, 1002–1020 (1990).
19. Bruland, K. W., Donat, J. R. & Hutchins, D. A. Interactive influences of bioactive trace metals on biological production in oceanic waters. *Limnol. Oceanogr.* **36**, 1555–1577 (1991).
20. Rich, H. R. & Morel, F. M. M. Availability of well-defined iron colloids to the marine diatom *Thalassiosira weissflogii*. *Limnol. Oceanogr.* **35**, 1555–1577 (1991).
21. Robinson, N. J., Procter, C. M., Connolly, E. L. & Guerinot, M. L. A ferric-chelate reductase for iron uptake from soils. *Nature* **397**, 694–697 (1999).
22. Eide, D. Molecular biology of iron and zinc uptake in eukaryotes. *Curr. Opin. Cell Biol.* **9**, 573–577 (1997).
23. Weinberg, E. D. Cellular regulation of iron assimilation. *Q. Rev. Biol.* **64**, 261–290 (1989).
24. Brand, L. E. Minimum iron requirements of marine phytoplankton and the implications for the biogeochemical control of new production. *Limnol. Oceanogr.* **36**, 1756–1771 (1991).
25. Sunda, W. G. & Huntsman, S. A. Iron uptake and growth limitation in oceanic and coastal phytoplankton. *Mar. Chem.* **50**, 189–206 (1995).
26. Boyd, P. W. & Newton, P. P. Does planktonic community structure determine downward particulate organic carbon flux in different oceanic provinces? *Deep-Sea Res.* **1** **46**, 63–91 (1999).
27. Lewis, B. L. *et al.* Voltammetric estimation of iron(III) thermodynamic stability constants for catecholate siderophores isolated from marine bacteria and cyanobacteria. *Mar. Chem.* **50**, 179–188 (1995).
28. Hutchins, D. A., DiTullio, G. R., Zhang, Y. & Bruland, K. W. An iron limitation mosaic in the California upwelling regime. *Limnol. Oceanogr.* **43**, 1037–1054 (1998).
29. Hudson, R. J. M. & Morel, F. M. M. Distinguishing between extra- and intracellular iron in marine phytoplankton. *Limnol. Oceanogr.* **34**, 1113–1120 (1989).
30. Schmidt, M. A. & Hutchins, D. A. Size-fractionated biological iron and carbon uptake along a coastal to offshore transect in the NE Pacific. *Deep-Sea Res.* **II** **46**, (1999).

Acknowledgements. We thank D. Kirchman, W. Sunda, S. Wilhelm, Y. Zhang and the captain and crew of the RV *Cape Henlopen*. This work was supported by the US NSF Biological and Chemical Oceanography (D.A.H., A.E.W. and G.W.L.), NIH, and California Sea Grant (A.B.).

Correspondence and requests for materials should be addressed to D.A.H. (e-mail: dahutch@udel.edu).

Tracking the evolution of insecticide resistance in the mosquito *Culex pipiens*

Thomas Lenormand*, Denis Bourguet*, Thomas Guillemaud* & Michel Raymond

Laboratoire Génétique et Environnement, Institut des Sciences de l'Évolution (UMR 5554), Université Montpellier II, 34095 Montpellier Cedex 5, France

The evolution of pesticide resistance provides some of the most striking examples of darwinian evolution occurring over a human life span. Identification of resistance alleles opens an outstanding framework in which to study the evolution of adaptive mutations from the beginning of pesticide application^{1–3}, the evolution of interactions between alleles (dominance⁴) or between loci (epistasis^{5,6}). Here we show that resistance alleles can also be used as markers to dissect population processes at a microevolu-

tionary scale. We have focused on the antagonistic roles of selection and migration involved in the dynamics of local adaptation with reference to allelic frequencies at two resistance loci in the mosquito *Culex pipiens*. We find that their frequencies follow an annual cycle of large amplitude (25%), and we precisely unravel the seasonal variation of migration and selection underlying this cycle. Our results provide a firm basis on which to devise an insecticide treatment strategy that will better control the evolution of resistance genes and the growth of mosquito populations.

Geographic gradients in allele frequency ('clines') in natural populations can be analysed using migration–selection models^{7,8} to obtain estimates of migration rates and selection coefficients^{9–13}. This powerful method works well for populations near equilibrium, such as hybrid zones¹⁴ that are considered to be "windows on evolutionary processes"¹⁵. The same method (which assumes equilibrium) can be applied to clines shaped by a balance between natural selection and gene flow across a variable environment^{7,8,16,17}, although such local adaptation may be much less stable over time (for example, see ref. 18). This approach has been used to analyse the cases of insect melanism^{19,20} and heavy-metal tolerance in plants²¹. We have used this framework to analyse insecticide resistance but have developed a method that does not require *ad hoc* hypotheses such as neutrality and genetic equilibrium and allows us to study the dynamics through time.

We sampled 8,600 *C. pipiens* mosquitoes during the breeding season (April to October) and the overwintering period (November to March) (Table 1). Sampling was done on ten dates from July 1995 to March 1997 along a north–south transect across organophosphate treated and non-treated areas in Southern France (Fig. 1). In *C. pipiens*, two major loci confer organophosphate resistance. Resistance alleles at the *Ace.1* locus code for a modified acetylcholinesterase (the organophosphate target), whereas those at the *Ester* locus code for overproduced detoxifying esterases^{22–24}. Alleles at these two loci were identified for each individual using a biochemical test and starch-gel electrophoresis, respectively^{22–24}.

We analysed fitness differences within and between loci, ignoring small differences between resistance alleles at the same locus which

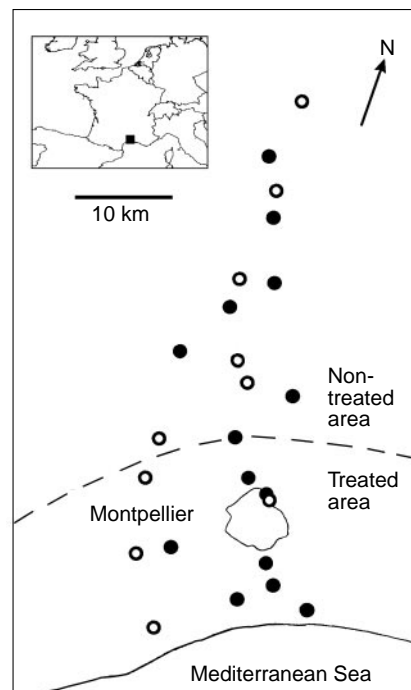


Figure 1 Sample site locations in the north–south transect in Southern France. Diapausing females were sampled in overwintering sites (caves; circles) and larvae or pupae were sampled in larval breeding sites (pools; filled circles). The dashed line indicates the boundary between the treated and non-treated areas.

* Present addresses: Department of Zoology, University of British Columbia, Vancouver V6T1Z4, Canada (T.L.); Station de Recherche de Lutte Biologique, INRA La Minière, 78 285 Guyancourt, France (D.B.); Lab. de biologia molecular, UCTRA, Universidade do Algarve, 8000 Faro, Portugal (T.G.).

Table 1 Sampling dates, number of sampled sites and sample sizes

Models		Descriptive				Migration-selection	
Sample set	Pop	<i>N</i>	Deviance	%TD	Deviance	%TD	
Oct. 1997	Breeding sites	8	52.2 (12)	0.86*	54.2	0.84	
Nov. 1995	Overw. sites	10	14.9 (14)	0.68*	28.4	0.40	
Nov. 1996	Overw. sites	10	9.4 (14)	0.89*	30.8	0.72	
Feb. 1996	Overw. sites	17	23.1 (21)	0.82*	65.3	0.51	
March 1997	Overw. sites	7	14.9 (11)	0.71*	34.8	0.33	
April 1996	Breeding sites	7	25.1 (11)	0.60*	39.3	0.38	
May 1996	Breeding sites	6	48.1 (10)	0.80*	60.4	0.75	
June 1996	Breeding sites	5	5.4 (2)	0.94*	7.4	0.85	
July 1995	Breeding sites	10	41.7 (14)	0.94*	52.3	0.92	
Aug. 1996	Breeding sites	7	20.1 (11)	0.89*	23.2	0.87	
All samples		87	254.7 (120)	0.88*	396.1 (15)	0.82	

Pop, number of sampled sites; *N*, sample size. The residual deviance, the number of degrees of freedom used (in parentheses), and the explained part of the total deviance (%TD) are shown for both the cline descriptive analysis and the migration-selection model.

* A significant decrease of resistance alleles from the coast was detected using descriptive models ($P < 0.001$).

have been estimated separately in longer-term studies^{23,25}. Individuals were pooled into classes {E}/{}O and {R}/{}S for the presence/absence of at least one resistance allele at the *Ester* (E) and the *Ace.1* (R) locus, respectively. The phenotypes were therefore treated as being {S,O}, {S,E}, {R,O} or {R,E}.

For each sampling date, we found a significant decrease of {R} and {E} frequency with distance from the coast (Table 1) using a descriptive model (see Methods). We also found that the cline shape followed an annual cycle: cline shape differed across seasons and was almost identical within seasons from one year to the next (Fig. 2). These clines can be interpreted as the consequence of local adaptation in a finite environment where migration and selection act as antagonistic forces¹⁷. A one-dimensional cline can be maintained at an equilibrium across a finite treated and non-treated area when resistance alleles confer a constant relative fitness advantage in the presence of insecticide but a relative fitness disadvantage (referred to as the 'cost' of resistance) in its absence². Also, it is required that the intensity of selection and the size of the treated area are large enough relative to the intensity of gene flow^{17,24}. For more than one locus, each cline is modified by the indirect selection due to linkage disequilibria and these conditions are more easily met²⁶.

Our data provide a rare opportunity to go beyond these snapshot pictures and to estimate migration and selection coefficients as well as their variation across time. We analysed the annual cycle of the clines as a consequence of annual variation in insecticide applications and alternations between breeding and overwintering seasons. We performed a maximum likelihood analysis (see Methods) using deterministic equations describing migration and selection to infer the allelic distribution at each step of the cycle and assuming the whole cycle is stable. One-dimensional clines were simulated using a series of demes connected by migration (see Methods). Some of the parameters required, such as the recombination rate (14.5%) between the *Ace.1* and *Ester* loci, and the size of the treated area ($L = 20$ km) were estimated from external data²⁴. Frequencies were computed separately for each sex during overwintering as only females overwinter as adults, whereas males survive as spermatozoa in fertilized females. The cycle was divided into nine intervals (between each sampling date: Fig. 3), within which selection and migration parameters are estimated, $p_i = (s_a, s_e, c_a, c_e, \Delta)$. Parameters s and c correspond to the selection coefficients due to insecticide treatments and the cost of resistance, respectively. The subscripts refer to loci (a for *Ace.1* and e for *Ester*); Δ is the migration distribution characterized by a mean (μ) and a variance (σ^2).

The best-fitting parameters explained 82% of the total deviance (the deviance is -2 times the log-likelihood) over the annual cycle, and the fit of each cline was close to the goodness of fit from purely descriptive models (88%), although 8 times more parsimonious (only migration and selection parameters are estimated; see Table 1). According to these results, the cycle can be divided into five stages

(Fig. 3). During stage I (when insecticides are applied), selection coefficients due to insecticide treatments are positive (for example, $s_a = 0.33$, $s_e = 0.19$ in summer), causing the frequencies of resistance alleles to increase in the treated area. The clines become steeper owing to the antagonistic effect of selection due to insecticide treatments and the cost of resistance (for example, $c_a = 0.11$ and $c_e = 0.07$ in summer) despite the homogenizing effect of strong migration ($\sigma = 6.6$ km generation^{-1/2}). At the end of this stage, migration-selection equilibrium is not completely reached (estimates of selection assuming the cline of July 1995 was at equilibrium²⁴ were therefore underestimated for both loci, about 0.01 for fitness cost and 0.03 for insecticide selection). Stage II corresponds to the end of the breeding season in the absence of insecticide ($s_a = s_e = 0$); the clines start to decay as a result of fitness costs ($c_a = 0.11$ and $c_e = 0.05$) and gene flow ($\sigma = 6.6$ km generation^{-1/2}). Stage III corresponds to an intense ($\sigma = 14.6$ km generation^{-1/2}) and directional ($\mu = 12.4$ km towards North) migration to the overwintering sites which strongly homogenizes frequencies and creates high positive linkage disequilibria (3–5%) along the transect, as expected. This asymmetrical migration explains the surprising increase in resistance alleles in the non-treated area for both loci in both November 1995 and 1996 (see also ref. 27). During the overwintering period (stage IV), resistance

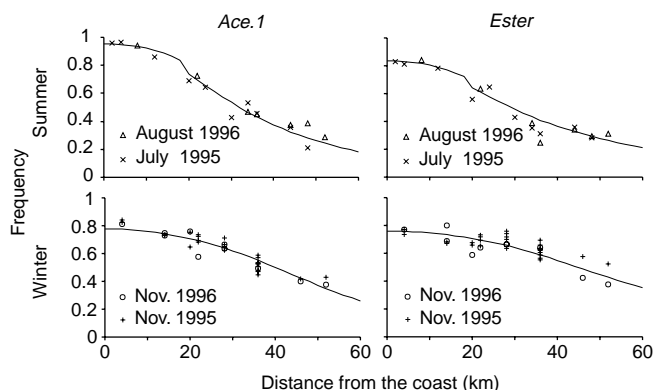


Figure 2 Summer and winter cline frequencies of 1995 and 1996. {R} frequency for *Ace.1* locus and {E} frequency for *Ester* locus are indicated as functions of distance from the coast in kilometres. Symbols represent observed frequencies and lines represent the clines fitted using the migration-selection model (see text). During the treatment periods in summer, resistance alleles are selected for in the treated area, producing the steep clines and high frequency of resistance alleles. Owing to the cost of resistance and gene flow, this frequency decreases when the treatments are interrupted, leading to shallow clines and lower frequencies of resistance alleles in winter. The occurrence and stability of this annual cycle are strong evidence that insecticide treatments and the cost of resistance act as antagonistic selective pressures.

alleles decrease in frequency owing to severe fitness costs ($c_a = 0.51$, $c_e = 0.26$) in the absence of movement ($\mu = \sigma = 0$) of diapausing females. Previous estimates of costs associated with *Ace.1* from local empirical data were similarly high ($c_a = 0.63$)^{22,27}. The last stage (V) corresponds to the first spring generation where resistance alleles increase even in the absence of insecticides. This increase is due to winter fitness costs on resistance alleles being higher in females than in spermatozoa (only an indirect selection operates on spermatozoa through the correlation between genotypes of assorted males and females). The net effect of natural selection over the whole winter is therefore expected to be approximately half of that estimated on females, which agrees well with our estimates (c_a and c_e estimated from the beginning of overwintering to the first spring generation were found to be 52 and 51%, respectively, of those estimated over the overwintering period).

A precise understanding of the conditions under which insecticide resistance occurs is necessary for the development of successful management strategies²⁸. Precise estimates of the migration distribution and costs of resistance allow us to compute a critical area of insecticide application below which resistance alleles fall to extinction²⁸. Using our results, this area is about half the actual area of treatment for resistance alleles of organophosphate insecticides. Unrelated insecticides such as *Bacillus sphaericus* could then

be used on the remaining part to achieve the same treated area size but without the evolution of organophosphate resistance. □

Methods

Descriptive cline models. The frequency cline of resistance alleles at locus *i* and time *j* was fitted according to a scaled negative exponential^{23,25}, $h_{ij} \exp(-a_{ij}x^2)$, where *x* is the distance from the coast, h_{ij} the maximum frequency of resistance alleles at locus *i* and time *j*, and a_{ij} is the rate of decrease of resistance alleles. Distributions of phenotypes were computed using allelic distributions²⁵, assuming that each locus was at Hardy–Weinberg equilibrium and allowing for linkage disequilibria in each population. The likelihood of a sample was computed from the phenotypic multinomial distribution and maximized for parameter estimation.

Migration–selection simulations. One-dimensional clines were simulated on a lattice. We used a binomial migration distribution reflected at one edge of the lattice to take into account the presence of the sea^{25,27}. Denoting the number (0, 1 or 2) of resistance alleles as *A* and *E* for the *Ace.1* and *Ester* loci, respectively, the fitness of an individual was computed as

$$1 - g(x) \left[\frac{s_a}{2} (2 - A) + \frac{s_e}{2} (2 - E) \right] - \frac{c_a A}{2} - \frac{c_e E}{2},$$

where $g(x) = 1$ for $x < 20$ km (treated zone) and zero otherwise. Co-dominance was assumed for insecticide resistance and for the cost of resistance, and epistasis between loci was neglected⁶. The order of the life cycle was assumed to be reproduction–migration–selection. Algorithms of migration and selection were checked using analytical results for one locus¹⁷. The number of generations corresponding to each stage of the cycle is indicated in Fig. 2 and is based on field estimations of generation time (B.D., G.T., C. Chevillon and R.M., manuscript in preparation).

Maximum likelihood estimation. Let n_{ijk} and g_{ijk} be the number and expected frequency of individuals having phenotype *i* in population *j* at time *k*. Then, the log-likelihood of observing all the data is

$$\sum_i \sum_j \sum_k n_{ijk} \times \ln(g_{ijk}),$$

where the expected frequencies of phenotypes (g_{ijk}) were computed using a large enough number of iterations of the annual cycle to ensure its stability. Maximum likelihood estimates of parameters were computed simultaneously using the Metropolis algorithm adapted from Barton¹⁰. Model selection was performed using the Akaike information criterion corrected for overdispersion (QAIC = scaled deviance + 2 × degrees of freedom)²⁹. The scaling factor is the ratio of residual deviance over residual degrees of freedom.

Received 26 March; accepted 16 June 1999.

- Mallet, J. The evolution of insecticide resistance: have the insects won? *Trends Ecol. Evol.* **4**, 336–340 (1989).
- McKenzie, J. A. *Ecological and Evolutionary Aspects of Insecticide Resistance* (Landes, Austin, 1996).
- Mutéro, A., Pralavorio, M., Bride, J. M. & Fournier, D. Resistance-associated point mutations in insecticide-insensitive acetylcholinesterase. *Proc. Natl Acad. Sci. USA* **91**, 5922–5926 (1994).
- Bourguet, D., Lenormand, T., Guillemaud, T., Marcel, V. & Raymond, M. Variation of dominance of newly arisen adaptive genes. *Genetics* **147**, 1225–1234 (1997).
- Davies, A. G. *et al.* *Scalloped wings* is the *Lucilia cuprina* *Notch* homologue and a candidate for the *Modifier* of fitness and asymmetry of diazinon resistance. *Genetics* **143**, 1321–1337 (1996).
- Raymond, M., Heckel, D. & Scott, J. G. Interaction between pesticide genes: model and experiment. *Genetics* **123**, 543–551 (1989).
- Haldane, J. B. S. The theory of a cline. *J. Genet.* **48**, 277–284 (1948).
- May, R. M., Endler, J. A. & McMurtrie, R. E. Gene frequency clines in the presence of selection opposed by gene flow. *Am. Nat.* **109**, 659–676 (1975).
- Barton, N. H. The structure of the hybrid zone in *Uroderma bilobatum* (Chiroptera: Phyllostomataidae). *Evolution* **36**, 863–866 (1982).
- Szymura, J. M. & Barton, N. H. Genetic analysis of a hybrid zone between the fire-bellied toads, *Bombina orientalis* and *Bombina variegata*, near Cracow in southern Poland. *Evolution* **40**, 1141–1159 (1986).
- Mallet, J. *et al.* Estimates of selection and gene flow from measure of clines width and linkage disequilibrium in *Heliconius* hybrid zones. *Genetics* **124**, 921–936 (1990).
- Sites, J. W., Barton, N. H. & Reed, K. M. The genetic structure of a hybrid zone between two chromosome races of the *Sceloporus grammicus* complex (Sauria, Phrynosomatidae) in central Mexico. *Evolution* **49**, 9–36 (1995).
- Porter, A. H., Wenger, R., Geiger, H., Scholl, A. & Shapiro, A. M. The *Pottia daphidice-edusa* hybrid zone in northwestern Italy. *Evolution* **51**, 1561–1573 (1997).
- Barton, N. H. & Hewitt, G. M. Adaptation, speciation and hybrid zones. *Nature* **341**, 497–503 (1989).
- Harrison, R. G. in *Oxford Surveys in Evolutionary Biology* (eds Antonovics, J. & Futuyma, D.) 69–128 (Oxford University Press, Oxford, 1990).
- Slatkin, M. Gene flow and selection in a cline. *Genetics* **75**, 733–756 (1973).
- Naglaki, T. Conditions for the existence of clines. *Genetics* **80**, 595–615 (1975).
- Cook, L. M., Dennis, R. L. H. & Mani, G. S. Melanic morph frequency in the peppered moth in the Manchester area. *Proc. R. Soc. Lond. B* **266**, 293–297 (1999).

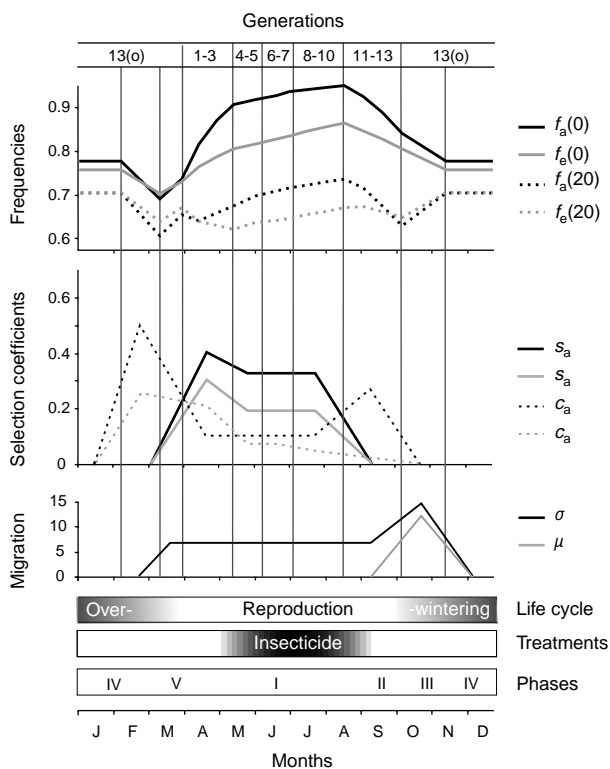


Figure 3 Annual variation of frequency clines at *Ace.1* (subscript *a*) and *Ester* (subscript *e*) fitted by the migration–selection model. These clines are represented by their frequency on the coast, $f(0)$, and at 20 km from the coast, $f(20)$. Corresponding seasonal variation of selection coefficients per generation due to insecticide treatments (*s*) and cost of resistance (*c*) as well as migration distribution mean (μ) and standard deviation (σ) in km are indicated. Vertical lines indicate dates of sampling. The number of generations considered between each of them is indicated on the top. The overwintering generation is indicated by (o) after the generation number. These estimates correspond to the best migration–selection model (that is, after model simplification). Each value represented is significantly different from zero and from other adjacent values on the graph of the same parameter. The cycle can be interpreted in five phases: insecticide treatment (I), end of the breeding season in the absence of treatment (II), migration to overwintering sites (III), overwintering (IV) and first spring generation (V).

19. Kettlewell, H. B. D. & Berry, R. J. The study of a cline. *Heredity* **16**, 403–414 (1961).
20. Mani, G. S. A theoretical study of morph ratio clines with special reference to melanism in moths. *Proc. R. Soc. Lond. B* **B210**, 299–316 (1980).
21. Jain, S. K. & Bradshaw, A. D. Evolutionary divergence among adjacent plant populations. I. The evidence and its theoretical analysis. *Heredity* **21**, 407–441 (1966).
22. Chevillon, C., Bourguet, D., Rousset, F., Pasteur, N. & Raymond, M. Pleiotropy of adaptive changes in populations: comparisons among insecticide resistance genes in *Culex pipiens*. *Genet. Res. Camb.* **70**, 195–204 (1997).
23. Guillemaud, T. *et al.* Evolution of resistance in *Culex pipiens*: allele replacement and changing environment. *Evolution* **52**, 443–453 (1998).
24. Lenormand, T., Guillemaud, T., Bourguet, D. & Raymond, M. Evaluating gene flow using selected markers: a case study. *Genetics* **149**, 1383–1392 (1998).
25. Lenormand, T., Guillemaud, T., Bourguet, D. & Raymond, M. Appearance and sweep of a gene duplication: adaptive response and potential for a new function in the mosquito *Culex pipiens*. *Evolution* **52**, 1705–1712 (1998).
26. Slatkin, M. Gene flow and selection in a two locus system. *Genetics* **81**, 787–802 (1975).
27. Lenormand, T. & Raymond, M. Analysis of clines with variable selection and variable migration. *Am. Nat.* (in the press).
28. Lenormand, T. & Raymond, M. Resistance management: the stable zone strategy. *Proc. R. Soc. Lond. B* **265**, 1985–1990 (1998).
29. Anderson, D. R., Burnham, K. P. & White, G. C. AIC model selection in overdispersed capture-recapture data. *Ecology* **75**, 1780–1793 (1994).

Acknowledgements. We thank C. Chevillon, I. Chuine, T. Day, P. David, P. Jarne, M. Kirkpatrick, J. Lagnel, Y. Michalak, S. Otto, N. Pasteur, F. Rousset and M. Whitlock for helpful comments and discussion, and C. Bernard and M. Marquie for technical assistance. This work was financed in part by GDR 1105 du programme Environnement, Vie et Sociétés du CNRS, by the PNETOX and by the Entente Interdépartementale pour la Démoustication du Languedoc Roussillon. T.L. was supported by an ASC fellowship from INRA contribution ISEM 99.068.

Correspondence and requests for materials should be addressed to T.L. (e-mail: lenorm@zoology.ubc.ca).

Illusory shifts in visual direction accompany adaptation of saccadic eye movements

Dan O. Bahcall & Eileen Kowler

Department of Psychology, Rutgers University, Piscataway, New Jersey 08854, USA

A central problem in human vision is to explain how the visual world remains stable despite the continual displacements of the retinal image produced by rapid saccadic movements of the eyes. Perceived stability has been attributed to ‘efferent-copy’ signals, representing the saccadic motor commands, that cancel the effects of saccade-related retinal displacements^{1–6}. Here we show, by means of a perceptual illusion, that traditional cancellation theories cannot explain stability. The perceptual illusion was produced by first inducing adaptive changes in saccadic gain (ratio of saccade size to target eccentricity). Following adaptation, subjects experienced an illusory mislocalization in which widely separated targets flashed before and after saccades appeared to be in the same place. The illusion shows that the perceptual system did not take the adaptive changes into account. Perceptual localization is based on signals representing the size of the initially-intended saccade, not the size of the saccade that is ultimately executed. Signals representing intended saccades initiate a visual comparison process used to maintain perceptual stability across saccades and to generate the oculomotor error signals that ensure saccadic accuracy.

Saccadic adaptation was produced conventionally^{7–11}. Subjects made a single saccade to look at a target point that stepped abruptly to an eccentric horizontal location, 228, 240 or 252 arcmin away. The background was dark; only the target was visible. Saccades were accurate, as expected^{11,12} (Fig. 1a). In the adaptation trials, which began after 20 baseline step-tracking trials, the target hopped either forwards or backwards by 48 arcmin (about 20% of the size of the original step) during the saccade. (Forward and backward hops, and rightward and leftward saccades, were tested in separate experimental sessions.) Saccades landed near the original

(pre-hop) target location during the first few adaptation trials (Fig. 1b). Adaptive changes occurred over the ensuing trials, when saccades began to land closer to the target’s final, post-hop position (Fig. 1c).

After adaptation reached nearly asymptotic levels, ‘probe’ trials were introduced to assess the perceived relative location of targets flashed before and after the saccade^{13–17} (Fig. 1d). A probe trial was run after every three consecutive adaptation trials, thus allowing saccades to remain in the adapted state. The saccadic target in probe trials was flashed for 100 ms. The display remained dark during the saccade to the remembered location of the flash. Two-hundred-and-fifty milliseconds after saccade detection, the post-saccadic probe target was flashed for 100 ms. The subject reported whether the post-saccadic probe was located to the left or to the right of the pre-saccadic target. We used a double-random staircase procedure (see Methods) to select the post-saccadic probe location according to the response on the immediately preceding probe trial, with the goal of ‘zooming in’ on the location that perceptually matched the remembered location of the pre-saccadic target.

Figure 2 (open symbols) shows the mean sizes of saccades to the right and left over successive blocks of 20 trials for the three subjects (two naive; one author) during forward, backward and no-hop (control) sessions. Saccadic gain (saccade size/target step size) was similar across the three target step sizes (228, 240 and 252 arcmin) so data from the three step sizes was combined (see Methods). Saccadic adaptation reached maximum levels after about 20–60 adaptation trials. The maximum levels of adaptation were less than hop size, and dependent on subject, saccadic direction and hop

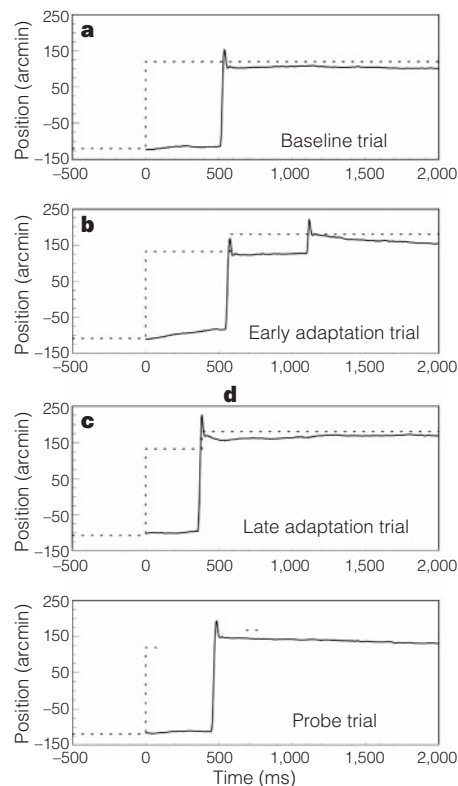


Figure 1 Representative traces of horizontal eye (solid line) and stimulus position (dotted line). Negative values are left of centre. **a**, Saccade in response to a 240-arcmin target step. Saccade size is the difference between pre- and post-saccadic eye position, bypassing the overshoot at the end of the saccade (see Methods). **b**, An early adaptation trial, 48-arcmin forward hop. **c**, A later adaptation trial. **d**, Probe trial, with pre- and post-saccadic flashes to be compared. Because of the intervening saccade, the pre-saccadic target and post-saccadic probe occupied different retinal loci.